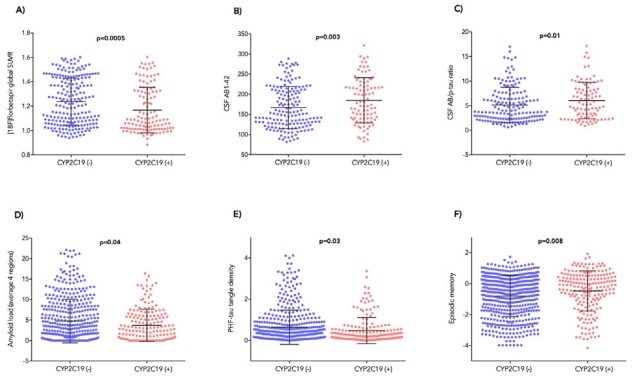

Figure 1. Comparison between non-carriers(-) and carriers(+) of the minor allele of rs4388808 (CYP2C19). A significant difference was observed in brain amyloid load (A), CSF Aβ levels (B) and CSF Aβ/p-tau ratio (C) using ADNI cohort. Results were generalized using post-mortem data from Rush ROS and MAP cohorts, where a concordant pattern was observed in amyloid load (D), PHF-tau tangle density (E) and episodic memory scores (F). The linear models were adjusted for age, gender and ApoE-e4 carriage status.

the brain, they modulate blood-flow regulation, metabolize cholesterol, and participate in neuroinflammatory processes. CYP activity is also implicated in Alzheimer's disease (AD), particularly in amyloid-β (Aβ) accumulation in CSF. We examined whether genetic polymorphisms of CYP are associated with AD pathology. **Methods:** [18F]florbetapir-PET imaging was employed to assess brain Aβ levels in 256 subjects from a discovery cohort (ADNI: 186CN, 105 lMCI, 47AD). Linear regression models examined the association of 30 SNPs from four genes of CYP (CYP3A4, CYP2C9, CYP2C19 and CYP1A1) with global [18F]florbetapir-SUVR, adjusting for age, sex, and ApoE-e4carriage status. Significant signals were interrogated at the voxel level using RMINC-tool, and, separately, tested for associations with CSF Aβ and Aβ/p-tau ratio. Neuropathologic data from the Rush ROS and MAP cohorts were used to generalize the findings to Aβ load and PHFtau tangle density by immunocytochemistry in post-mortem brains (302 CN, 180 aMCI, 259 AD). **Results:** The analysis of [18F]florbetapir identified an intronic variant in the CYP2C19 gene (rs4388808; P=0.0005), in which carriers of the minor-allele (G) had lower global SUVR (Figure 1). The voxel-wise analysis showed a significant effect of the SNP in the frontal and posterior cingulate cortices, as well as in the inferior parietal cortex (Figure 2). Carriers of the minor-allele were also associated with higher CSF Aβ (P=0.003) and higher Aβ/p-tau ratio (P=0.01). In post-mortem brains, minor-allele carriers had a lower Aβ load (P=0.04), lower PHFtau tangle density (P=0.03) as well as better episodic memory (P=0.008). **Conclusions:** The rs4388808, an intronic variant of the CYP2C19 gene is implicated in Aβ load, tau pathology and episodic memory, where the minor-allele protects against AD pathology.

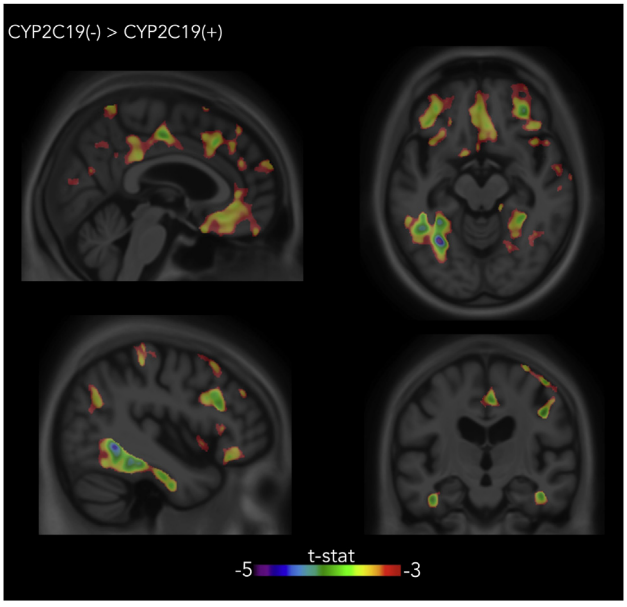

Figure 2. Voxel-wise comparison between minor allele non-carriers(-) and carriers(+) of the polymorphism rs4388808 of CYP2C19. A significant difference was observed in the frontal and posterior cingulate cortices, as well as in the inferior parietal cortex. The voxel-wise analysis was adjusted for age, gender and ApoE-e4 carriage status.

IC-P-030 *IN VIVO* NADH FLUORESCENCE IMAGING OF DOUBLE TRANSGENIC AD MICE REVEALS CHRONIC TISSUE HYPOXIA

Bistra Iordanova, Matthew C. Murphy, William E. Klunk, Alberto L. Vazquez, *University of Pittsburgh, Pittsburgh, PA, USA.*
Contact e-mail: bei3@pitt.edu

Background: Vascular and metabolic dysfunctions are well known features of Alzheimer's disease (AD) and they precede clinical dementia. Undoubtedly vascular changes are expected as amyloid accumulates in the arterial vessel walls in cerebral amyloid angiopathy (CAA), leading to the death of smooth muscle cells, cerebral hypoperfusion and inadequate oxygen supply. These vascular events could also contribute to metabolic alterations in glucose homeostasis. High resolution *in vivo* study of the dynamic vascular and metabolic events may reveal which tissue regions and cell populations are affected and cast light on the mechanisms that contribute to AD pathogenesis. **Methods:** We used fluorescence imaging of nicotinamide adenine dinucleotide (NADH) as an intrinsic marker for cellular metabolic states and tissue oxygen supply *in vivo*. We resolved the tissue boundaries of NADH fluorescence in the cortex of transgenic AD mice (B6C3.Tg(APPswe-PSEN1de9), n=4, 12-24 months old) and observed NADH pattern relative to vessels during hyperoxia and normoxia. We then used *in vivo* two-photon fluorescence microscopy together with cell-type specific labeling to determine the cellular origin of the intrinsic signal and the locality of CAA. **Results:** Reduction of oxygen supply from hyperoxia to normoxia produced no detectable changes in controls, however AD mice showed characteristic NADH pattern (Figure 1A), indicative of reduced oxygen gradient and rise in glycolysis in tissues further away from the arterial oxygen supply. Areas around capillary beds showed decreased NADH signal. Two-photon imaging under the same conditions revealed numerous cells with increased signal (Figure 1B) and only some of those cells stained positive for the astrocyte marker Sulforhodamine-101 (Figure 1C). All AD mice had CAA and tissue plaques seen with Methoxy-X04 staining (Figure 1D) and there appeared to be no association of the NADH signal with the plaques location. **Conclusions:** In agreement with previous findings, double transgenic AD mice display chronic tissue hypoxia. Our preliminary results also

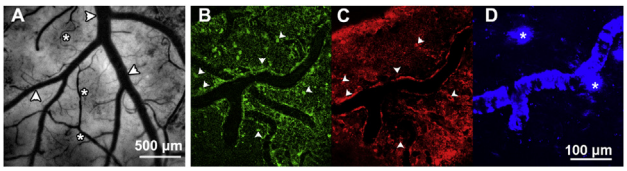

Figure 1. *In vivo* NADH fluorescence imaging of AD mice reveals chronic tissue hypoxia and cellular metabolic shift. A) Characteristic NADH pattern after reduction of oxygen supply. Arrowheads pointing to a vein; asterisks at arteries. B) Two-photon imaging under the same conditions shows numerous cells with increased signal (green). C) A subset of those cells stain positive for the astrocyte marker SR101 (red). Arrowheads at cells double positive for NADH and SR101. D) Cortex also shows heavy CAA (blue) and tissue plaques (blue, asterisks).

indicate that under those conditions a subset of cells may adapt by up-regulating glycolysis to overcome the deficient oxidative phosphorylation. The population of cells with increased NADH signal is likely a combination of neurons and glia. This work can lead to new strategies that target metabolic pathways to halt AD progression.

IC-P-031 APPLICATION OF DOUBLE MR IMAGING TO DETECT AMYLOID OLIGOMERS IN THE BRAIN OF APP/PS1 TRANSGENIC MODEL MICE

Ikuo Tooyama[1], Daijiro Yanagisawa[1], Hiroyasu Taguchi[1], Tomoko Kato[1], Koichi Hirao[2], Nobuaki Shirai[3], Takayuki Sogabe[4], Shigehiro Morikawa[1], *[1]Shiga University of Medical Science, Otsu, Japan; [2]Northeastern Industrial Research Center of Shiga Prefecture, Nagahama, Japan; [3]Industrial Research Center of Shiga Prefecture, Nagahama, Japan; [4]Otsuka Pharmaceutical Co., Ltd, Kawauchi-cho, Japan. Contact e-mail: kinchan@belle.shiga-med.ac.jp*

Background: We have developed two types of potential imaging agents using ^{19}F-MRI: ^{19}F-containing styrylbenzoxazole derivative (Shiga-X22) and curcumin derivative (Shiga-Y5). Shiga-Y5 detects both Aβ oligomers and Aβ aggregates, while Shiga-X22 only detects Aβ aggregates. Thus, the Shiga-Y5 images subtracted by Shiga-X22 may reflect the images of Aβ oligomers. In this study, we applied double MR probe-imaging to detect amyloid oligomers in the brain of APPswe/PS1dE9 double transgenic model mice. **Methods:** All experimental procedures were approved by the Animal Care and Use Committee of our University. Six APPswe/PS1dE9 double transgenic mice at age of 20-month-old were used. We simultaneously injected Shiga-Y5 and Shiga-X22 at a dose of 200 mg/kg into the tail vein of three mice. At 3-h after the injection, ^{19}F chemical shift imaging was obtained using a 7-tesla MR scanner. Another three mice were killed by overdose of sodium pentobarbital and we removed the brain. Then, the concentrations of Aβ oligomers were measured by enzyme-linked immunosorbent assay (ELISA). **Results:** The ^{19}F MR signal of Shiga-Y5 appeared mainly in the olfactory bulb, the subcortical area, and the cerebellum. In contrast, the ^{19}F MR signal of Shiga-X22 displayed predominantly in the olfactory bulb, the cortex, and the cerebellum. Then, we produced a subtracted image by subtracting ^{19}F MR images of Shiga-X22 from that of Shiga-Y5. ^{19}F MR signal in the subtracted image was located in the subcortical area. ELISA measurement showed that Aβ oligomers uniformly distributed in the brain except for the brainstem, and there is no specific region showing the accumulation of Aβ oligomers. In contrast, the level of insoluble Aβ was significantly less in the subcortical area where the concentration of insoluble Aβ was relatively low. The imbalance between relative high level of Aβ oligomers and the less level of insoluble Aβ in the subcortical area may contribute to intense ^{19}F MR signal in the subtracted image. **Conclusions:** We employed double probe MR images using Shiga-Y5 and SHiga-X22 to detct Aβ oligomers in the brain of AD model mouse.

IC-P-032 *IN VIVO* TWO-PHOTON IMAGING OF THE EFFECTS OF TAUOPATHY AND AMYLOIDOPATHY ON SYNAPSE DYNAMICS IN THE RTG4510 AND J20 TRANSGENIC MODELS RESPECTIVELY

Johanna Jackson, *Eli Lilly and Co. Ltd., Windlesham, United Kingdom. Contact e-mail: jackson_johanna@lilly.com*

Background: A progressive loss of synapses occurs at the early clinical stages of Alzheimer's Disease (AD) and has been correlated with cognitive deficits in AD patients. However, it is relatively unknown how synapse dynamics are affected by the two main pathological hallmarks of AD; the intracellular accumulation of tau and the extracellular accumulation of amyloid β protein, Here we used *in vivo* two-photon microscopy to assess the temporal dynamics of axonal boutons and dendritic spines in transgenic mouse models of human tauopathy (rTg4510) and amyloidopathy (J20). The Tg4510 model expresses the P301L tau mutation downstream of a tetracycline-operon-responsive element, whilst the J20 expresses both the *Indiana* (V717F) and *Swedish* (K670N, M671L) mutation on the amyloid precursor protein gene. **Methods:** Following a craniotomy, adeno-associated virus expressing green fluorescent protein (GFP) was injected into layer 2/3 of the somatosensory cortex to enable the visualisation of neurons and a cranial window was implanted for long-term imaging. GFP-labelled neurons were imaged in Tg4510s, J20s and wild-type littermate controls during a time period which spanned the onset of pathology. The gross morphology of axons and dendrites and the dynamics of their synaptic structures were assessed as the pathology progressed. In the rTg4510 experiments, a third group of animals received doxycycline to determine the effects of suppressing the pathogenic P301L transgene. In the J20 experiments, the density and size of amyloid plaques and the effects of plaque proximity on synapse density were also assessed. **Results:** In rTg4510s, gross morphological changes such as the presence of dystrophic neurites were visible as the tauopathy progressed and these were found to have a distinctive morphological phenotype prior to neurite degeneration. Alongside this, synapse instability and loss were also observed and could be prevented by suppressing the P301L transgene. In J20 animals, amyloid plaques increased in size and density over time and spine density was affected by the dendrite's proximity to plaques. **Conclusions:** Both tauopathy and amyloidopathy had effects on synapses as the respective pathology progressed. These results will inform subsequent drug discovery studies to identify novel therapies to stabilize synapse loss in AD.

IC-P-033 RESTING-STATE NETWORK DYSFUNCTION IN ALZHEIMER'S DISEASE: A SYSTEMATIC REVIEW AND META-ANALYSIS

AmanPreet Badhwar[1,2], Angela Tam[1,3,4], Christain Dansereau[1,2], Pierre Orban[1,2,4], Roberto Toro[5], Pierre Bellec[1,2], *[1]Centre for Research, Institute of Geriatric Medicine, Montreal, QC, Canada; [2]University of Montreal, Montreal, QC, Canada; [3]McGill University, Montreal, QC, Canada; [4]Centre for Studies on Prevention of Alzheimer's Disease (StoP-AD Centre), Douglas Mental Health Institute, Montreal, QC, Canada; [5]Institut Pasteur, Paris, France. Contact e-mail: amanpreet.badhwar@mail.mcgill.ca*